



Case Report

SCOLIOSIS IN MAINZER-SALDINO SYNDROME: A CASE REPORT AND REVIEW OF THE LITERATURE

S. Amico^{1*}, D. Scoscina¹, G. Facco¹, N. Specchia¹, A.P. Gigante¹ and M. Martiniani²

¹Department of Clinical and Molecular Sciences, Università Politecnica delle Marche, Ancona, Italy;

²Clinic of Adult and Paediatric Orthopaedics, Azienda Ospedaliero-Universitaria, Ospedali Riuniti di Ancona, Ancona, Italy

**Corresponding Author*

Silvia Amico, MD

Department of Clinical and Molecular Sciences,

Università Politecnica delle Marche,

Via Tronto 10/a,

60020 Torrette di Ancona, Italy

e-mail: s.amico@pm.univpm.it

ABSTRACT

Mainzer-Saldino Syndrome (MZSDS) is a rare autosomal recessive disease caused by mutations in gene IFT140 encoding intraflagellar transport protein, a subunit of the IFT-A complex involved in retrograde ciliary transport. MZSDS is a multisystem disorder characterized by chronic renal disease and skeletal abnormalities: phalangeal cone-shaped epiphyses, short stature, short-ribs thoracic dysplasia, pelvic deformities, maxillofacial and proximal epiphysis and femur metaphysis abnormalities. Scoliosis has never been described as one of the features of this syndrome. We present the case of 26-year-old Italian Caucasian man affected by MZSDS with a severe scoliosis surgically treated. Cobb angle of major thoracic curve was 120° and Cobb angle of major lumbar curve was 110°. Curve flexibility was evaluated on the preoperative standing lateral bending X-ray and side-bending X-ray. By means of CT images, we obtained a Three-Dimensional (3D) model of spine used for the preoperative study. A single-posterior spinal arthrodesis extending from T2 to L5 vertebrae was performed. No intraoperative and early postoperative surgical complications occurred. Postoperative radiographs demonstrated main thoracic correction from 120° to 56° (53.7% correction rate), main lumbar correction from 110° to 52° (52.7% correction rate). In conclusion, our hypothesis is that scoliosis may be a skeletal feature of MZSDS. It can produce a severe deformity needing for major surgical treatment. Preoperative multidisciplinary assessment is necessary. Scoliosis correction and maintenance at follow-up result in the improvement of pulmonary function and high patient satisfaction.

KEYWORDS: *posterior spinal fusion, case report, spinal deformities, MZSDS, 3D printing*

Received: 16 January 2023

Accepted: 24 February 2023

ISSN 1973-640

Copyright © by BIOLIFE 2023

This publication and/or article is for individual use only and may not be further reproduced without written permission from the copyright holder. Unauthorized reproduction may result in financial and other penalties. **Disclosure: All authors report no conflicts of interest relevant to this article.**

INTRODUCTION

Mainzer-Saldino Syndrome (MZSDS) is a rare autosomal recessive disease caused by mutations in gene IFT140 encoding intraflagellar transport protein, a subunit of the IFT-A complex involved in retrograde ciliary transport (1). Its prevalence is unknown. MZSDS is a multisystem disorder characterized by phalangeal cone-shaped epiphyses (PCSE) and chronic renal disease. Occasional features are: retinal dystrophy, cerebellar ataxia, hepatic fibrosis, bilateral hearing difficulties and skeletal abnormalities, suggesting that MZSDS is a skeletal ciliopathy (2). Skeletal abnormalities are: short stature, short-ribs thoracic dysplasia, pelvic deformities, maxillofacial and proximal epiphysis and femur metaphysis abnormalities. Diagnosis occurs when children have develop kidney failure – usually between the ages of 10 and 14. Electroretinography supports the diagnosis. Genetic testing (sequence analysis of the entire coding region of IFT140) is essential. In the past, the disease was burdened by a relatively high mortality rate, mainly due to renal insufficiency that quickly evolved into end-stage renal disease. The remarkable improvements recorded in the field of kidney transplantation have drastically reduced the mortality from renal syndrome (3).

Scoliosis has never been described as one of the features of this syndromic condition. In this article, we report the first described case of severe scoliosis associated with MZSDS requiring surgical treatment. Spinal deformities and medical conditions in syndromic population affect complication rates significantly.

CASE PRESENTATION

We present the case of 26-year-old Italian Caucasian man affected by MZSDS with a severe scoliosis surgically treated. The diagnosis of MZSDS was performed on the basis of clinical features and genetic testing when he was 9-years-old.

The patient was born by spontaneous delivery, at term, from healthy parents with normal stature and body build. He was the second of three children. The oldest brother died when he was a teenager because of renal failure in MZSDS, while the youngest is unaffected. Prenatal echography had not revealed any growth failure. At birth no abnormalities were detected. There was no family history of scoliosis.

At 4 years, progressive bilateral valgus knees arose. Physical and radiological examination of the knees carried out at 7 years showed worsening painful knees after long walking, and valgus angle equal to 12° on right and 15° on left. The patient underwent corrective surgery by bilateral femoral epiphysiodesis with good result. Two years later, removal of staple was performed.

At 9 years, because of acidosis with reduced glomerular filtration, he underwent renal biopsy that diagnosed focal segmental glomerulonephritis. Later the patient developed stage V renal insufficiency requiring hemodialysis treatment. Consequently he had hypertensive heart disease, anemia, hyperparathyroidism and osteoporosis. Furthermore he had chronic liver disease with splenomegaly, retinitis pigmentosa and respiratory failure.

At 10 years, scoliosis was evidenced and it was first treated with global postural rehabilitation and brace but the patient had low compliance. Subsequently to scoliotic curves progression, surgical treatment became necessary but the patient and his family refused.

At 12 years, the patient underwent bilateral flat feet surgical correction.



Fig 1. Preoperative (a, b, c, d) clinical photographs show the severity of spine deformity at the clinical examination and clinical photographs at 2 years follow up (e, f, g, h) show good overall balanced spine in the coronal and sagittal planes.

In 2016 the patient was placed on waiting kidney transplant list at the Department of Nephrology of Riuniti Hospital in Ancona, but three years later he was excluded because of the development of severe respiratory failure.

In July 2019 the patient came to our attention and it seemed appropriate to proceed with surgical correction. On February 2020 he was admitted to Clinical Orthopaedics of Riuniti Hospital in Ancona. He was 155 cm tall and he had low BMI equal to 14.8. Physical examination showed deformity of the back, waistline asymmetry, unequal shoulder and anterior superior iliac spine levels. The Adam's forward bend test revealed right rib hump and left lumbar prominence. The assessment of posture and gait detected listing to left side due to leg length discrepancy with right leg 2.5 cm longer than left leg, clinically measured (Fig. 1).

No skin or soft tissue abnormalities were noted overlying his spine. Neurological examination confirmed no apparent current vascular and nervous deficits in his upper and lower limbs. F5 muscle strength was evaluated using MRC (Medical Research Council) Scale. Tendon reflexes were symmetrically elicited (Fig. 1)

The patient underwent brain and spine magnetic resonance imaging (MRI) before surgery in order to evaluate the presence of spinal cord malformation including occult syrinx, spinal stenosis, spinal cord tumors, Arnold-Chiari malformations or neuromuscular disorders (4).

Cobb angle measurement of coronal curves and coronal balance were achieved on standing posteroanterior X-ray (Fig. 2).

Rightward major thoracic curve extending from T4 to T11 with T8 apical vertebra, leftward major lumbar curve extending from T12 to L5 with L2 apical vertebra and leftward minor cervical curve extending from C5 to T3 with T1 apical vertebra were revealed. Measurement of pelvic obliquity (PO) was equal to 12°, right side elevated (5) (Fig. 3).

The Risser grade was 5 indicating his final skeletal growth. Sagittal curve and sagittal balance were determined on standing lateral X-ray (6). Curve flexibility was evaluated on the preoperative standing lateral bending X-ray and side-bending X-ray. In Table I, there is a recap of radiographic coronal measures on preoperative time.

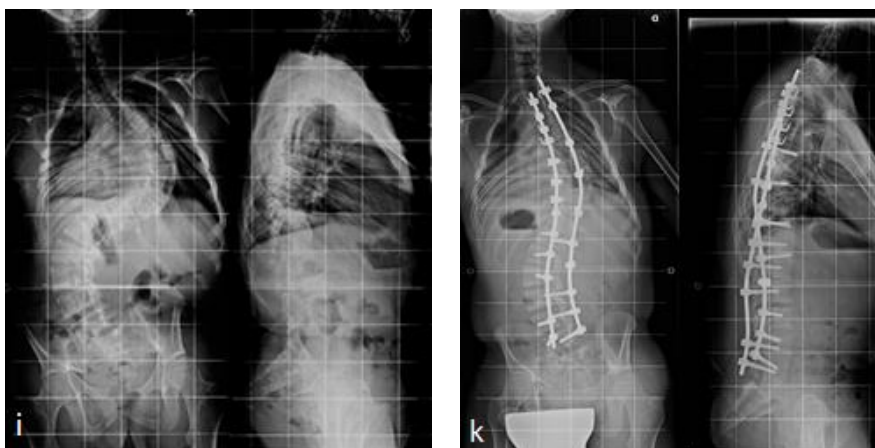


Fig. 2. Preoperative posteroanterior and lateral X ray examinations show the severity of scoliotic curves (i) and postoperative posteroanterior and lateral X ray examinations show a satisfactory correction of the spine deformity (k)

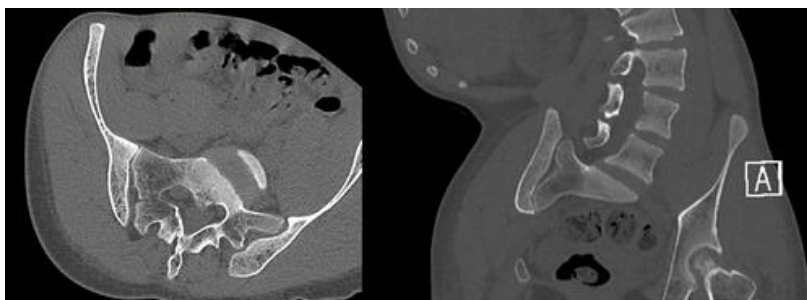


Fig 3. Computed tomography (CT) images show the rotation of sacrum and pelvis obliquity (PO).

Computed tomography scan with reconstruction according to the axial plane of each vertebra and with 3D reconstruction was performed to evaluate dystrophic features.

According to the classification system proposed by Li Y et al, on a total of 34 pedicles, evaluated on CT images with reconstruction according to the axial plane of each vertebra, the results were: A: 10; B: 13; C: 11; D: 0; E: 0 (7). Wedging of vertebral bodies is present in six vertebrae at the apices of the major curves. According to Ho et al method, rotation was assessed on CT images with reconstruction according to the axial plane of the apical vertebra (8, 9). The rotation angle of T8 was 38°, the rotation angle of L2 was 59°.

During the hospitalization, a preoperative assessment was organized. The patient underwent anesthesiological evaluation which required specialist investigations. Echocolordoppler of the supra-aortic vessels and the venous lower limbs detected no steno-obstructive diseases. High-grade restrictive spirometry pattern and high DLCO reduction were observed. Cardiological evaluation detected an estimated PAPs equal to 43 mmHg secondary to restrictive pneumopathy.

Preoperative planning

The patient underwent spine and pelvis CT, by whose images we obtained a Three-Dimensional (3D) model, which was thereafter printed by using a fused deposition modeling printer (Fig. 4).

8 hours were spent for software production of the 3D printed model, while the printing required 175 hours. The amount of costs for materials was about 300 Euros (10).

Surgical time

A single-posterior spinal arthrodesis extending from T2 to L5 vertebrae was performed. Intraoperative spinal cord monitoring was performed during the surgical time recording somatosensory and motor evoked potentials and the signal was always normal.



Fig. 4. *Three-Dimensional (3D) printed model was used in preoperative planning.*

A subperiosteal exposure of the spine with extensive facetectomies was performed in order to further mobilise the curves. Posterior instrumentation was hybrid and it included laminar and pedicle hooks, sublaminar bands, pedicle screws and rods. During the procedure for inserting hybrid instrumentation, the surgeons noticed a reduced bone quality, especially of the pedicles. At first, a temporary titanium rod on thoracic curve concavity from T2 to T12 was used (Fig. 5).

Corrective manoeuvres included apical segmental translation, rod derotation and proximal/distal distraction of the construct. Later, a cobalt-chrome rod on the right-side was placed from T2 to L5. The correction of the thoracic convexity was achieved using compression manoeuvres while the correction of the lumbar concavity was achieved using apical

Table I. *Radiographic coronal measures on preoperative time (T0).*

| | Thoracic curve (°) | Lumbar curve (°) | Coronal imbalance (cm) |
|--------------------------|-----------------------|---------------------|---------------------------|
| Before surgery (T0) | 120 | 110 | -2 |
| Standing lateral bending | 100 | 95 | - |
| Side-bending | 84 | - | - |

segmental translation, rod derotation and proximal/distal distraction manoeuvres. At last, temporary titanium rod was removed and a cobalt-chrome rod on left-side was placed from T2 to L5. The rods were attached tightly to spine by hybrid instrumentation (11). Locally harvested bone from the spinous processes was used to achieve interfacetal and intertransverse arthrodesis. It was supplemented by freeze-dried bone allograft.

The total operative time was about 12 hours. Total amount of blood loss was 2000 mL. Intraoperatively the patient underwent hemodialysis.

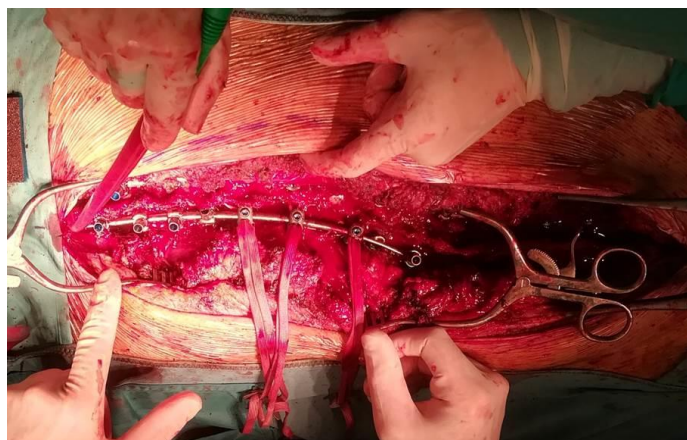


Fig 5. Temporary titanium rod on thoracic curve concavity used during the surgical procedure to perform corrective manoeuvres.

Postoperative time

Postoperatively, the patient was monitored at the postoperative intensive care unit (ICU). The day after, he was extubated and transferred to Orthopaedics Clinic.

During the initial postoperative period, there were no neurological abnormalities and no sign of respiratory dysfunction. There was no sign of wound infection. On the 5th postoperative day, he mobilised out of bed with walking frame.

Postoperative radiographs demonstrated main thoracic correction from 120° to 56° (53.7% correction rate), main lumbar correction from 110° to 52° (52.7% correction rate) with a persistent imbalanced spine in the coronal and sagittal planes. The measures are reported in Table II and Table III (Fig. 2).

Leg length discrepancy equal to 2.5 cm persisted and it was corrected by uniform heel-to-toe plateau on the left foot. The patient was discharged on the 10th postoperative day. No intraoperative and early postoperative surgical complications occurred.

Follow-up

In the third postoperative month, he returned to his daily activities. Radiographs of his spine at latest follow-up 2 years after surgery demonstrated a satisfactory maintenance of surgical correction in the coronal and sagittal planes. No late postoperative surgical complications occurred (Fig. 1). The spirometry at 2-years follow-up noticed high-moderate-grade restrictive pattern with FVC improved from 41% of predicted to 56% of predicted and a moderate reduction in DLCO

Table II. Radiographic coronal measures on preoperative time (T0), postoperative time (T1) and 2-years follow-up (FU).

| | Thoracic curve (°) | Lumbar curve (°) | Coronal imbalance (cm) |
|------------------------|-----------------------|---------------------|---------------------------|
| Before surgery (T0) | 120 | 110 | -2 |
| After surgery (T1) | 56 | 52 | -6.4 |
| 2-years follow-up (FU) | 57 | 54 | +0.5 |

Table III. Radiographic sagittal measures on preoperative time (T0), postoperative time (T1) and 2-years follow-up (FU).

| | Kyphosis (°) | Lordosis (°) | Sagittal imbalance (cm) |
|------------------------|-----------------|-----------------|----------------------------|
| Before surgery (T0) | 43 | 50 | +2.5 |
| After surgery (T1) | 25 | 28 | +6.5 |
| 2-years follow-up (FU) | 29 | 29 | + 3.7 |

(47% of predicted). The comparison of preoperative and 2-years follow-up pulmonary functions is shown in Table IV. SRS-24 questionnaire was administered to assess the patient’s clinical satisfaction in 2-year follow-up (12) (Fig. 6). The results are recapped in Table V (Fig. 6).

Table IV. SRS-24 questionnaire results

| Domain | Score Pt/Possible (max) |
|---------------------------|-------------------------|
| Pain | 32/35 |
| General self-image | 13/15 |
| Self-image after surgery | 14/15 |
| Function after surgery | 10/10 |
| General function | 12/15 |
| Function-activity | 14/15 |
| Satisfaction with surgery | 14/15 |
| Total | 109/120 |
| 90,8% | |

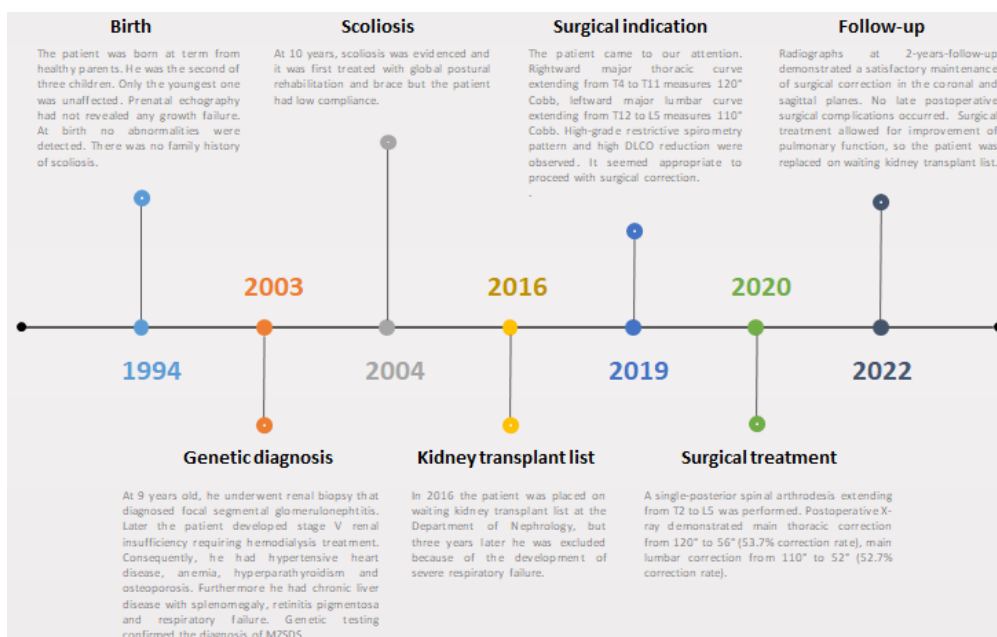


Fig. 6. The timeline shows the key events of the our case.

Table V. SRS-24 questionnaire results.

| Domain | Score Pt/Possible (max) |
|---------------------------|-------------------------|
| Pain | 32/35 |
| General self-image | 13/15 |
| Self-image after surgery | 14/15 |
| Function after surgery | 10/10 |
| General function | 12/15 |
| Function-activity | 14/15 |
| Satisfaction with surgery | 14/15 |
| Total | 109/120 |
| 90,8% | |

Consent

Written informed consent was obtained by the patient for publication of this case report and any accompanying images. A copy of the written consent is available for review by the editor of this journal.

DISCUSSION

The term “syndromic scoliosis” is used to describe scoliosis associated with a systemic disease. Scoliosis in Ehler Danlos syndrome (EDS), Marfan syndrome (MF), Down syndrome, Achondroplasia (AP), Prader-Willi Syndrome (PWS), and Osteogenesis Imperfecta are representative of this category. Syndromic population has a greater rate of developing scoliosis than idiopathic population. This article focuses on the analysis of the literature regarding the outcomes of surgical management in syndromic scoliosis patients. In a recent study of 2019, Andrew S. Chung et al. compared the hospital outcomes and surgical trends of patients with syndromic scoliosis and patients with idiopathic scoliosis undergoing spinal fusion. There was a significant decline in the number of anterior approaches performed in both cohorts, whereas the number of posterior approaches increased. Rates of major complications (Neurologic injury and pulmonary embolism) were 3-times higher in syndromic scoliosis cohort. Similar findings were reported in procedural and device-related complications (13). Levy et al. reviewed the literature and noted high rates of postoperative infections (5%), implant failures (20%), and pseudoarthrosis (25%) in the syndromic scoliosis population (3). These results are in line with existing literature (14, 15).

Mainzer-Saldino Syndrome (MZSDS) is a multisystemic disease characterized by bony development disorders. Scoliosis has never been described in literature as one of the features of this syndrome. We reported the first described case of severe scoliosis associated with MZSDS requiring surgical treatment.

In a recent review, Li X. et al. summarized the role of primary cilia and ciliary proteins in the pathogenesis of skeletal diseases including scoliosis. In this review, the authors showed evidence that the primary cilia may be a promising target of clinical intervention for skeletal diseases (osteoporosis, bone/cartilage tumor, osteoarthritis, intervertebral disc degeneration, spine scoliosis, and other cilium-related skeletal diseases) (16). Schlösser et al. reported that the prevalence of scoliosis and significant spinal asymmetry in 198 patients affected by primary ciliary dyskinesia was 8 and 23%, respectively (17).

Our patient was first noted at the age of 25 years. He was affected by a severe spine deformity which required major scoliosis surgery.

3D printed model permitted to study and exhaustively comprehend the complexity of the deformity: we could have the visual and tactile experience of the entity of curves, sagittal and coronal balances, pelvis rotation, pedicles dimension and position. The 3D printed model was so used to evaluate vertebral dystrophy, in particular pedicles, allowing us to identify the type of surgical approach and to choose the better position of hooks, screws and sublaminar bands. It was useful to reduce the fluoroscopy exposition for both surgeons and the patient. The 3D printed model was also an instrument for better explaining the operative planning of this complex deformity to patients and younger surgeons.

A single-stage posterior deformity correction was managed. According to Dobbs MB et al., posterior-only approach has the advantage of providing the same correction as an anterior/posterior spinal fusion, without the need for entering the thorax and more negatively impacting pulmonary function (18). The posterior-only approach performed using high-density hybrid instrumentations (implant density equal to 0.72) produced a satisfactory correction of the severe deformity (19).

Operative time and intraoperative blood loss were compatible with the greater complexity of the surgery. Motor and sensory traces recorded intraoperatively were unchanged throughout the procedure.

The coronal and sagittal imbalance did not improve on immediate postoperative time, probably due to the severe impact of the surgical trauma, but it decreased in the 2-year follow-up leading to an acceptable overall balance.

Curves measurements on postoperative time and on the follow-up demonstrate no loss of surgical correction across the instrumented levels. There was also no evidence of detected pseudoarthrosis and no add-on junctional deformity proximally or distally the levels of the spinal fusion. Instrumentation was in side.

Surgical treatment allowed for improvement of pulmonary function, so the patient was replaced on waiting kidney transplant list at the Department of Nephrology of Riuniti Hospital in Ancona.

As SRS-24 questionnaire showed, surgical treatment positively impacted patient's life quality: no experience of severe pain, better rating of his self-image, no limitations in daily activities, walking without fatigue, practicing moderate sport.

The clinical case described in this paper was an important challenge for orthopaedic surgeons. Because of the serious comorbidities a detailed planning of each phase was essential, from the preoperative preparation of the patient, to the surgical procedure, up to the postoperative care and monitoring over time and follow-up. A multidisciplinary approach was the key of the success of the surgical treatment. Surgeons approaching a rare syndrome should fully understand its complexity. In addition to meticulous surgical planning, the patient must be accompanied and supported during all stages of care.

CONCLUSIONS

In conclusion, our hypothesis is that scoliosis may be a skeletal feature of MZSDS. It can produce a severe deformity needing for major surgical treatment. Surgical correction of scoliosis restores spinal balance, prevents severe pulmonary and cardiological complications and mechanical back pain, as well as improves cosmesis. Because of severe comorbidities, preoperative multidisciplinary assessment is necessary to avoid surgical morbidity. Scoliosis correction and maintenance at follow-up result in the improvement of pulmonary function and high patient satisfaction. Given the paucity of existing data regarding deformity correction outcomes in syndromic scoliosis population, further researches are necessary for a better management of these conditions.

ACKNOWLEDGMENTS

The authors would like to thank Health Physics Department, Ospedali Riuniti di Ancona for the support in 3D model production process.

REFERENCES

1. Perrault I, Saunier S, Hanein S, et al. Mainzer-Saldino syndrome is a ciliopathy caused by IFT140 mutations. *Am J Hum Genet.* 2012;90(5):864-870. doi:<https://doi.org/10.1016/j.ajhg.2012.03.006>
2. Oud MM, Latour BL, Bakey Z, et al. Cellular ciliary phenotyping indicates pathogenicity of novel variants in IFT140 and confirms a Mainzer-Saldino syndrome diagnosis. *Cilia.* 2018;7(1). doi:<https://doi.org/10.1186/s13630-018-0055-2>
3. Levy BJ, Schulz JF, Fornari ED, Wollowick AL. Complications associated with surgical repair of syndromic scoliosis. *Scoliosis.* 2015;10(14). doi:<https://doi.org/10.1186/s13013-015-0035-x>
4. Sanguinetti C, Specchia N, Gigante A, de Palma L, Greco F. Clinical and pathological aspects of solitary spinal neurofibroma. *J Bone Joint Surg Br.* 1993;75(1):141-147. doi:<https://doi.org/10.1302/0301-620X.75B1.8421013>
5. Banno T, Yamato Y, Hasegawa T, et al. Impact of pelvic obliquity on coronal alignment in patients with adolescent idiopathic scoliosis. *Spine Deform.* 2020;8(6):1269-1278. doi:<https://doi.org/10.1007/s43390-020-00145-x>
6. Liu RW, Teng AL, Armstrong DG, Poe-Kochert C, Son-Hing JP, Thompson GH. Comparison of supine bending, push-prone, and traction under general anesthesia radiographs in predicting curve flexibility and postoperative correction in adolescent idiopathic scoliosis. *Spine (Phila Pa 1976).* 2010;35(4):416-422. doi:<https://doi.org/10.1097/BRS.0b013e3181b3564a>
7. Li Y, Luo M, Wang W, et al. A Computed Tomography-Based Comparison of Abnormal Vertebrae Pedicles Between Dystrophic and Nondystrophic Scoliosis in Neurofibromatosis Type 1. *World Neurosurg.* 2017;106(898-904). doi:<https://doi.org/10.1016/j.wneu.2017.07.064>
8. Ho EK, Upadhyay SS, Chan FL, Hsu LC, Leong JC. New methods of measuring vertebral rotation from computed tomographic scans. An intraobserver and interobserver study on girls with scoliosis. *Spine (Phila Pa 1976).* 1993;18(9):1173-1177. doi:<https://doi.org/10.1097/00007632-199307000-00008>
9. Lam GC, Hill DL, Le LH, Raso JV, Lou EH. Vertebral rotation measurement: a summary and comparison of common radiographic and CT methods. *Scoliosis.* 2008;3(16). doi:<https://doi.org/10.1186/1748-7161-3-16>

10. Facco G, Massetti D, Coppa V, et al. The use of 3D printed models for the pre-operative planning of surgical correction of pediatric hip deformities: a case series and concise review of the literature. *Acta Biomed.* 2022;92(6):e2021221. doi:<https://doi.org/10.23750/abm.v92i6.11703>
11. Cinnella P, Rava A, Mahagna AA, Fusini F, Masse A, Girardo M. Over 70 degrees thoracic idiopathic scoliosis: Results with screws or hybrid constructs. *J Craniovertebr Junction Spine.* 2019;10(2):108-113. doi:https://doi.org/10.4103/jcvjs.JCVJS_39_19
12. Haheer TR, Gorup JM, Shin TM, et al. Results of the Scoliosis Research Society instrument for evaluation of surgical outcome in adolescent idiopathic scoliosis. A multicenter study of 244 patients. *Spine (Phila Pa 1976).* 1999;24(14):1435-1440. doi:<https://doi.org/10.1097/00007632-199907150-00008>
13. Chung AS, Renfree S, Lockwood DB, Karlen J, Belthur M. Syndromic Scoliosis: National Trends in Surgical Management and Inpatient Hospital Outcomes: A 12-Year Analysis. *Spine (Phila Pa 1976).* 2019;44(22):1564-1570. doi:<https://doi.org/10.1097/BRS.0000000000003134>
14. Gjolaj JP, Sponseller PD, Shah SA, et al. Spinal deformity correction in Marfan syndrome versus adolescent idiopathic scoliosis: learning from the differences. *Spine (Phila Pa 1976).* 2012;37(18):1558-1565. doi:<https://doi.org/10.1097/BRS.0b013e3182541af3>
15. Rava A, Dema E, Palmisani M, Palmisani R, Cervellati S, Girardo M. Sublaminar fixation versus hooks and pedicle screws in scoliosis surgery for Marfan syndrome. *J Craniovertebr Junction Spine.* 2020;11(1):26-30. doi:https://doi.org/10.4103/jcvjs.JCVJS_12_20
16. Li X, Guo S, Su Y, et al. Role of Primary Cilia in Skeletal Disorders. *Stem Cells Int.* 2022;2022(6063423). doi:<https://doi.org/10.1155/2022/6063423>
17. Schlosser TPC, Semple T, Carr SB, et al. Scoliosis convexity and organ anatomy are related. *Eur Spine J.* 2017;26(6):1595-1599. doi:<https://doi.org/10.1007/s00586-017-4970-5>
18. Dobbs MB, Lenke LG, Kim YJ, Luhmann SJ, Bridwell KH. Anterior/posterior spinal instrumentation versus posterior instrumentation alone for the treatment of adolescent idiopathic scoliotic curves more than 90 degrees. *Spine (Phila Pa 1976).* 2006;31(20):2386-2391. doi:<https://doi.org/10.1097/01.brs.0000238965.81013.c5>
19. Clin J, Le Naveaux F, Driscoll M, et al. Biomechanical Comparison of the Load-Sharing Capacity of High and Low Implant Density Constructs With Three Types of Pedicle Screws for the Instrumentation of Adolescent Idiopathic Scoliosis. *Spine Deform.* 2019;7(1):2-10. doi:<https://doi.org/10.1016/j.jspd.2018.06.007>